Design of Audio Parametric Equalizer Filters Directly in the Digital Domain

Joshua D. Reiss, *Member, IEEE*

***Abstract*—Most design procedures for a digital parametric equalizer begin with analog design techniques, followed by applying the bilinear transform to an analog prototype. As an alternative, an approximation to the parametric equalizer is sometimes designed using pole-zero placement techniques. In this paper, we present an exact derivation of the parametric equalizer without resorting to an analog prototype. We show that there are many solutions to the parametric equalizer design constraints as usually stated, but only one of which consistently yields stable, minimum phase bbehaviorwith the upper and lower cutoff frequencies positioned around the center frequency. The conditions for complex conjugate poles and zeros are found and the resultant pole zero placements are examined.**

***Index Terms*—Filter design, parametric equalizers, peaking and notch filters, pole zero placement.**

I. Introduction

Many signal processing applications involve enhancing or attenuating only a small portion of a signal's frequency spectrum, while leaving the remainder of the spectrum unaffected. This effect is commonly obtained in audio applications by using a biquadratic filter that has a frequency response which is characterized by a boost or cut G around a specified center frequency ω_c. In digital audio equalization, any desired frequency response may be realized by cascading such filters with different center frequencies, which are then often referred to as parametric equalizer filters.

Apart from the center frequency, a parametric equalizer filter is also characterized by its bandwidth. Filters having a small bandwidth B relative to their center frequency (i.e., having a high Q-factor, defined as $Q = \omega_c / B$), are better known as notch and peaking (or resonance) filters.

The most common approach to digital filter design [1], [2] starts from the design of an analog filter, followed by a bilinear transform that maps the analog frequency axis $[0; 1)$ onto the digital frequency axis $[0, \omega_s/2]$, with ω_s the sampling frequency in radians. Many parametric equalizer design techniques use this approach with the digital design variables ω_c and B "prewarped" to analog variables, and are now well-established in the literature [3], [4]. These include the Direct form I (or Direct form II) [5], [6], and Allpass with feedforward form (using the Lattice or Normalized Ladder design) [7], [8]. In [9], it was shown that these methods all yield the same filter coefficients provided that the same definition of bandwidth is used in the design constraints. Thus filter performance, such as sensitivity to coefficient quantization or the susceptibility to limit cycles, is dependent on the implementation architecture, but not the derivation of the parametric equalizer's coefficients.

Both the generalized parametric equalizer [10] and the parametric equalizer with prescribed Nyquist frequency gain[11] attempt to introduce new parametric controls to compensate for asymmetric warping, but both methods continue to use analog design techniques to determine the target frequency response.

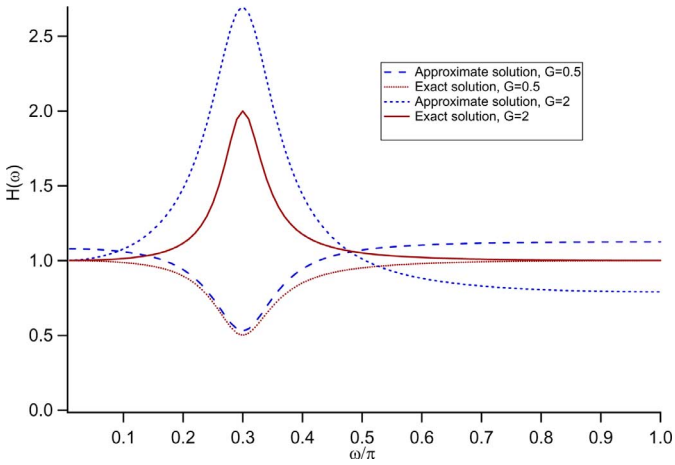

Fig. 1. Transfer functions for digital parametric equalizers designed using an exact solution based on an analog prototype, and an approximate solution using pole zero placement techniques. The normalized center frequency was 0.3π, bandwidth 0.1π, and gain of 0.5 or 2. For all cases, bandwidth was defined as in [17].

As an alternative to transformation of an analog design, filters are sometimes designed directly in the digital domain. For instance, an exact solution for digital Butterworth filter designs, without the need for an analog prototype, was achieved in [12]. Towards this goal, the parametric equalizer filter may be designed using pole-zero placement techniques. However, many of the solutions do not specify bandwidth [13], [14] and hence are not considered parametric, and some are limited only to ideal notch filter designs where the gain is set to zero [13], [15], [16]. To the best of this author's knowledge, only one fully digital parametric equalizer design technique has been presented [17]. Unfortunately, the approximations taken in this approach imply that the constraints are not exactly satisfied. In particular, this method places both poles and zeros at an angle ω_c, which ensures a poor approximation of both poles and zeros for high bandwidth, and poor approximation of the zeros for high gain. This is demonstrated in Fig. 1, which depicts the resultant transfer functions for parametric equalizers designed using the bilinear transform of an analog prototype, and using the approximate pole zero placement technique of [17]. It is clear that the pole zero placement technique produces a transfer function which does not accurately satisfy the constraints on bandwidth and gain.

In this paper, we derive the filter coefficients for the parametric equalizer directly in the digital domain, without the need for the bilinear transform or for any approximations. This approach has the benefits of being less cumbersome and more intuitive than to design a digital filter by first designing an analog one, and yet does not suffer from the errors introduced due to approximations introduced in existing pole zero placement techniques.

The paper is organized as follows. Section II presents the derivation of the parametric equalizer, leading to a large number of possible solutions. In Section III, the solutions are examined. We show that there are actually 32 possible solutions to the parametric equalizer design constraints as usually stated, but only one of these solutions consistently yields stable, minimum phase behavior with the upper and lower cutoff frequencies positioned around the center frequency. The conditions for which each solution is possible are explained, and the preferred solution is identified. In Section IV, this preferred solution is analyzed. The conditions for complex conjugate poles and zeros are found and the effect of modifying the gain, center frequency or bandwidth is explained

Manuscript received March 18, 2010; revised August 05, 2010; accepted October 25, 2010. Date of publication November 11, 2010; date of current version June 03, 2011. The associate editor coordinating the review of this manuscript and approving it for publication was Mr. James Johnston.

The author is with the Centre for Digital Music, Queen Mary University of London, London, E1 4NS, U.K. (e-mail: josh.reiss@eecs.qmul.ac.uk).

Color versions of one or more of the figures in this paper are available online at http://ieeexplore.ieee.org.

Digital Object Identifier 10.1109/TASL.2010.2091634

in terms of movement of poles and zeros on the complex plane. Conclusions and directions for future work are given in Section V.

II. Parametric Equalizer Design

A second-order biquadratic filter may be given in pole zero form as follows:

$$H(z) = c\frac{(z-q_1)(z-q_2)}{(z-p_1)(z-p_2)} = c\frac{1-(q_1+q_2)z^{-1}+q_1q_2z^{-2}}{1-(p_1+p_2)z^{-1}+p_1p_2z^{-2}} \quad (1)$$

where in this form we have not specified whether the poles and zeros exist as real values or complex conjugate pairs. Traditionally, the five filter coefficients are calculated so as to satisfy a set of five design equations

$$\begin{aligned} H(0) &= 1 \\ H(\pi) &= 1 \\ \left.\frac{d|H(\omega)|}{d\omega}\right|_{\omega_c} &= 0 \\ |H(\omega_c)| &= G \\ \omega_u - \omega_l &= B, \quad where \\ |H(\omega_u)| &= |H(\omega_l)| = G_B. \end{aligned} \quad (2)$$

In other words, the gain at DC and Nyquist is set to 1, there is a maximum or minimum of the magnitude response at the center frequency with corresponding gain G and there is a bandwidth B which is the distance between an upper and lower frequency where the gain is G_B. Setting the DC and Nyquist gain to be 1 facilitates the cascading of several parametric equalizer filters, and ensures that for narrow bandwidth, the frequency components far from the center frequency are unchanged. G_B is not an adjustable parameter. Instead there are several definitions which are used, some of which depend on G.

We thus have five constraints and an equation with five unknowns. We proceed by applying each constraint in (2) in turn to this filter, removing one unknown as each constraint is applied.

The first two constraints give

$$\boxed{\begin{aligned} c(q_1+q_2) &= p_1+p_2 \\ c(1+q_1q_2) &= 1+p_1p_2 \end{aligned}}. \quad (3)$$

In other words, you can completely define the poles in terms of the zeros, or vice versa.

The square magnitude of the filter may be given by

$$|H(\omega)|^2 = \frac{c^2[(1+q_1q_2)\cos\omega-(q_1+q_2)]^2+(1-q_1q_2)^2\sin^2\omega}{c^2[(1+q_1q_2)\cos\omega-(q_1+q_2)]^2+(2-c(1+q_1q_2))^2\sin^2\omega} \quad (4)$$

Using the chain rule, the third constraint reduces to

$$(1-c)[(1+q_1q_2)\cos\omega_c-(q_1+q_2)](1-cq_1q_2) \times[(q_1+q_2)\cos\omega_c-(1+q_1q_2)] = 0. \quad (5)$$

So we have four conditions that can lead to the derivative being 0. But if c equals 1 or $(q_1q_2)^{-1}$, then the square magnitude of the transfer function becomes uniformly one. So in general, these are not solutions.

We will now deal separately with the two remaining solutions to the third constraint.

Case 1:

$$\boxed{(1+q_1q_2)\cos\omega_c = q_1+q_2}$$

From (4), the fourth constraint becomes

$$\left.|H(\omega)|^2\right|_{\omega=\omega_c} = G^2 = \frac{c^2(1-q_1q_2)^2}{(2-c(1+q_1q_2))^2} \quad (6)$$

and hence this gives two possible solutions:

$$q_1q_2 = \frac{G(2-c)\pm_c c}{c(G\pm_c 1)}. \quad (7)$$

We retain the plus-minus sign and consider both solutions simultaneously. The $\pm$ signs are denoted with subscript c so that it is clear here and in the following formulas when they are dependent.

Using (7) to eliminate dependence on the zeros from (6), we find

$$|H(\omega)|^2 = \frac{(G\pm_c c)^2(\cos\omega-\cos\omega_c)^2+G^2(1-c)^2\sin^2\omega}{(G\pm_c c)^2(\cos\omega-\cos\omega_c)^2+(1-c)^2\sin^2\omega}. \quad (8)$$

We define

$$\alpha \equiv \sqrt{\frac{G^2-G_B^2}{G_B^2-1}}, \beta \equiv \alpha\frac{1-c}{G\pm_c c}. \quad (9)$$

So from (8) and the definition of the upper and lower cutoff frequencies in the fifth constraint of (2)

$$\beta^2 = \left[\frac{\cos\omega_l-\cos\omega_c}{\sin\omega_l}\right]^2 = \left[\frac{\cos\omega_u-\cos\omega_c}{\sin\omega_u}\right]^2. \quad (10)$$

Note that this also gives a constraint on the definition of G_B, $G^2 \geq G_B^2 \geq 1$ or $1 \geq G_B^2 \geq G^2$.

If G_B is defined using the arithmetic mean of the extremes of the square magnitude response, $G_B^2 = (1+G^2)/2$, then $G_B^2-1 = (G^2-1)/2 = G^2-G_B^2$, and thus the square root term α in the definition of β is equal to 1. This is thus the simplest definition, which also has the benefit that a boost and a cut by equal and opposite gains in dB, and equal bandwidth, cancel exactly, as described in [4] and [9].

Solving for c in the definition of β gives

$$\boxed{c = \frac{\alpha-\beta G}{\alpha\pm_c\beta}}. \quad (11)$$

Equation (10) implies that there are four possible choices for the relationship between β and the upper and lower cutoff frequencies We deal with these as two separate cases, each involving a $\pm$ sign.

Case 1.1:

$$\frac{\cos\omega_l-\cos\omega_c}{\sin\omega_l} = \frac{\cos\omega_c-\cos\omega_u}{\sin\omega_u} = \pm\beta.$$

The ω_c term can be eliminated to give

$$\beta = \pm\frac{\cos\omega_l-\cos\omega_u}{\sin\omega_l+\sin\omega_u} \quad (12)$$

where we assumed $\sin\omega_l \neq -\sin\omega_u$. Using trigonometric sum to product formulas

$$\beta = \pm\tan\left(\frac{B}{2}\right). \quad (13)$$

On the other hand, if $\sin\omega_l = -\sin\omega_u$, then $\omega_u = -\omega_l$. Mapping ω_u to $[0;2\pi]$, either ω_u is less than or greater than π. If $\omega_u < \pi$, our definition of bandwidth B implies $\omega_u = B/2$. So

$$\beta = \pm\frac{\cos\omega_c-\cos\left(\frac{B}{2}\right)}{\sin\left(\frac{B}{2}\right)}. \quad (14)$$

If $\omega_u > \pi$, then $\omega_u = \pi + B/2$. So

$$\beta = \pm\frac{\cos\omega_c - \cos\left(\pi + \frac{B}{2}\right)}{\sin\left(\pi + \frac{B}{2}\right)} = \mp\frac{\cos\omega_c + \cos\left(\frac{B}{2}\right)}{\sin\left(\frac{B}{2}\right)}. \quad (15)$$

Case 1.2:

$$\frac{\cos\omega_c - \cos\omega_l}{\sin\omega_l} = \frac{\cos\omega_c - \cos\omega_u}{\sin\omega_u} = \pm\beta.$$

Here, the approach used in Case 1.1 does not work, since trigonometric sum to product formulas do not reduce to terms involving bandwidth. Instead, we replace ω_u with $\omega_l + B$, and use sum of two angle formulas to break up terms involving the upper cutoff frequency. This case then becomes

$$\begin{aligned}\beta\sin\omega_l &= \pm(\cos\omega_c - \cos\omega_l)\\ \beta\sin\omega_l\cos B + \beta\cos\omega_l\sin B &= \pm(\cos\omega_c - \cos\omega_l\cos B\\ &\quad + \sin\omega_l\sin B). \end{aligned} \quad (16)$$

We can rewrite (16) as follows:

$$\begin{aligned}\sin\omega_l &= \frac{\cos\omega_c[(\cos B - 1) \pm \beta\sin B]}{(\beta^2+1)\sin B}\\ \cos\omega_l &= \frac{\cos\omega_c[\sin B \pm \beta(1-\cos B)]}{(\beta^2+1)\sin B}. \end{aligned} \quad (17)$$

Then, using $\cos^2\omega_l + \sin^2\omega_l = 1$

$$(\beta^2+1)^2\sin^2 B = (\beta^2+1)[\sin^2 B + (1-\cos B)^2]\cos^2\omega_c. \quad (18)$$

Solving for β gives

$$\beta = \pm\frac{\sqrt{\cos^2\omega_c - \cos^2\left(\frac{B}{2}\right)}}{\cos\left(\frac{B}{2}\right)}. \quad (19)$$

Note that the $\pm$ sign in (19) is different from the $\pm$ sign used to describe this case. However, we get the same two solutions, (19), regardless. Also, for β to be real, $\cos^2\omega_c \geq \cos^2(B/2)$. So, for $\omega_c > 0$, $B > 2\omega_c$ for this solution to hold.

Case 2:

$$(q_1 + q_2)\cos\omega_c = 1 + q_1 q_2.$$

The solutions to this case can be found using a similar procedure to that provided in Case 1, although the derivation becomes slightly more complicated. However, it is more illuminating to consider this case in terms of poles and zeros.

Suppose we consider one of the solutions to Case 1, and reflect a pole and a zero around the unit circle, and normalize the transfer function by this operation. Since complex poles or zeros occur only in complex conjugate pairs, this is only possible if the poles and zeros lie on the real axis. The new transfer function becomes

$$H' = c\frac{q_1}{p_1}\frac{(z - q_1^{-1})(z - q_2)}{\left(z - p_1^{-1}\right)(z - p_2)}. \quad (20)$$

It can be seen that H' obeys the first two constraints, and the square magnitude response reduces to

$$|H(\omega)|^2 = |H'(\omega)|^2 = \frac{(\cos\omega - \cos\omega_c)^2 + G^2\beta^2\sin^2\omega}{(\cos\omega - \cos\omega_c)^2 + \beta^2\sin^2\omega}. \quad (21)$$

Therefore, since the last three constraints only describe the magnitude response, and H and H' have the same (square) magnitude response, it follows that H' must also be a solution to the parametric equalizer.

If we divide the condition for Case 1 by q_1, we have

$$\left(q_1^{-1} + q_2\right)\cos\omega_c = 1 + q_1^{-1}q_2. \quad (22)$$

and hence Case 2 holds for H'. Similarly, if we reflect a pole and a zero for a Case 2 solution, then this represents a solution to Case 1. That is, this operation represents a bijective mapping between the sets of solutions to the two cases. So Case 2 must consist of all solutions to Case 1 where one pole and one zero are reflected through the unit circle.

III. Explicit Description of the Solutions

Our formulas for deriving the parametric equalizer are determined from the boxed equations previously. Equation (11) gives the gain term. Then from the condition for Case 1 and (7), we find the zeros:

$$q_{1,2} = \frac{\alpha\cos\omega_c \pm_{1,2}\sqrt{\beta^2G^2 - \alpha^2\sin^2\omega_c}}{\alpha - \beta G}. \quad (23)$$

Then from (3) and (11) we find the pole positions

$$p_{1,2} = \frac{\alpha\cos\omega_c \pm_{1,2}\sqrt{\beta^2 - \alpha^2\sin^2\omega_c}}{\alpha \pm_c \beta}. \quad (24)$$

And β is given in any of the following forms:

$$\begin{aligned}\beta = &\pm\tan\left(\frac{B}{2}\right),\\ &\pm\frac{\cos\omega_c + \cos\left(\frac{B}{2}\right)}{\sin\left(\frac{B}{2}\right)},\\ &\pm\frac{\cos\omega_c - \cos\left(\frac{B}{2}\right)}{\sin\left(\frac{B}{2}\right)},\ or\\ &\pm\sqrt{\frac{\cos(2\omega_c) - \cos B}{1 + \cos B}}. \end{aligned} \quad (25)$$

At this point, we should note that a similar procedure to that used above could have been applied to direct form, yielding the coefficients of the filter as functions of center frequency, gain, and bandwidth. However, the direct form derivation does not lend itself to easily explaining the solutions, as described in Section III-A.

A. Enumerating the Solutions

Consider the five constraints of (2). These each give conditions for the coefficients of (1) and the position of the upper and lower frequencies. The first two constraints give (3) in all cases. Then, the third constraint gives two solutions to (5), Case 1 and Case 2. If we consider Case 1, then (7) gives two solutions to the fourth constraint. In either case, (9) has four possible solutions. The first two solutions each have three solutions, (13) to (15), and the second two solutions to (9) each have two solutions, but these are the same in both cases, and given by (19). So, for Case 1, we have $2\cdot(2\cdot 3 + 1\cdot 2) = 16$ solutions.

Case 2 is all the solutions of Case 1, but with a zero and a pole reflected by the unit circle. Thus, in terms of different sets of coefficients, we have a total of 32 solutions.

All solutions can be explained in terms of poles and zeros. The $\pm$ signs in (25) determine if the zeros are inside or outside the unit circle, and then the $\pm_c$ sign in (24) determines if the poles are inside or outside the unit circle. If poles and zeros are on the real axis, then there are additional solutions (Case 2) where both a pole and a zero have been reflected across the unit circle. Thus, there are only a possible $32/4 = 8$ stable, minimum phase solutions.

For each choice of β, one could conceive of additional situations which give the same magnitude response where just one or three of the

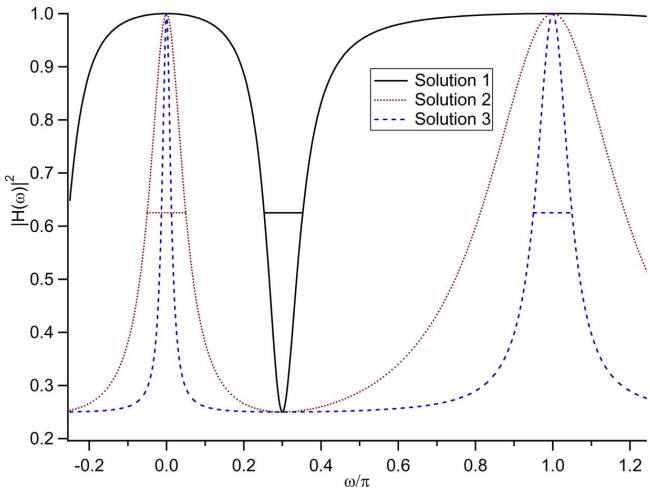

Fig. 2. Square magnitude of the transfer function for normalized center frequency 0.3π, gain of 0.5, and bandwidth 0.1π. Transfer functions and bandwidth locations are shown for the first three solutions (solid, dotted, and dashed line, respectively) for β.

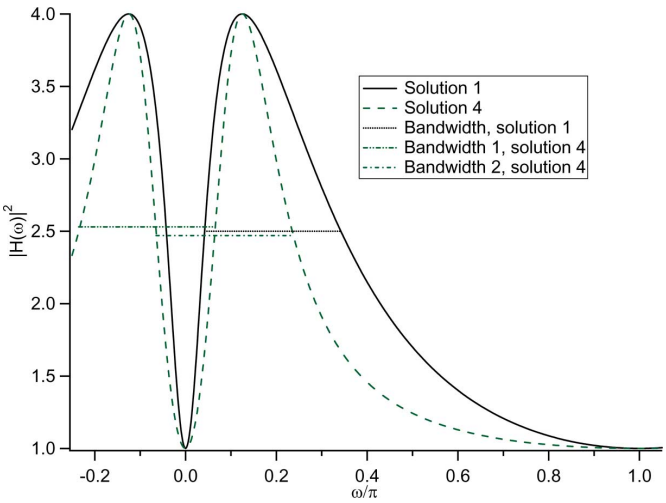

Fig. 3. Square magnitude of the transfer function for normalized center frequency 0.125π, gain of 2, and bandwidth 0.3π. Transfer functions and bandwidth locations are shown for the first and last solutions (solid line and dashed line, respectively) for β. The two possible bandwidth locations for the last solution have been offset slightly from $G_B = 2.5$ for clarity.

real valued poles and zeros are outside the unit circle, but these would violate the first two constraints of (2).

B. Explaining Solutions for β

It still remains to explain why there are multiple different solutions for β, especially since previous derivations of the parametric equalizer have only given solutions similar to $\tan(B/2)$. The reason comes from the fact that our bandwidth definition, even though it is commonly used, is still vague in its specification. It simply specifies the distance between two frequencies where the transfer function magnitude is G_B. However, for a notch (peaking) filter, these frequencies could be either side of where the magnitude response has its minimum (maximum), as is intended, or else they could be either side of where a notch (peaking) filter has its maximum (minimum). This is shown in Fig. 2, which depicts three possible square magnitude plots for center frequency 0.3π, gain of 0.5, and bandwidth 0.1π, where all units have been normalized such that half the sampling frequency is set to π. All three plots satisfy the parametric equalizer constraints. However, the dotted red plot, corresponding to the second option for β places the upper and lower cutoff frequencies around DC, and the dashed blue plot, corresponding to the third option for β places the upper and lower cutoff frequencies around half the sampling frequency.

Consider a parametric equalizer with center frequency 0.125π, gain of 2 and bandwidth $0.3\pi (Q = 5/12)$, again in normalized frequency units. Admittedly, such a low Q factor would not often be used. In Fig. 3, two possible plots of the square magnitude of the transfer function are depicted. These correspond to the first and fourth choices for β. The fourth solution has two possible placements of the bandwidth. Either both cutoff frequencies are located where the transfer function is rising, or both are located where the transfer function is falling. This explains why these solutions are only possible (the term under the square root in (19) must be positive) for large bandwidth, and why there are two solutions in (19), corresponding to the two different choices for placement of bandwidth.

IV. Preferred Solution

From the previous section, only the first solution for β, $\beta = \pm\tan(B/2)$, positions the upper and lower cutoff frequencies correctly on either side of the center frequency.

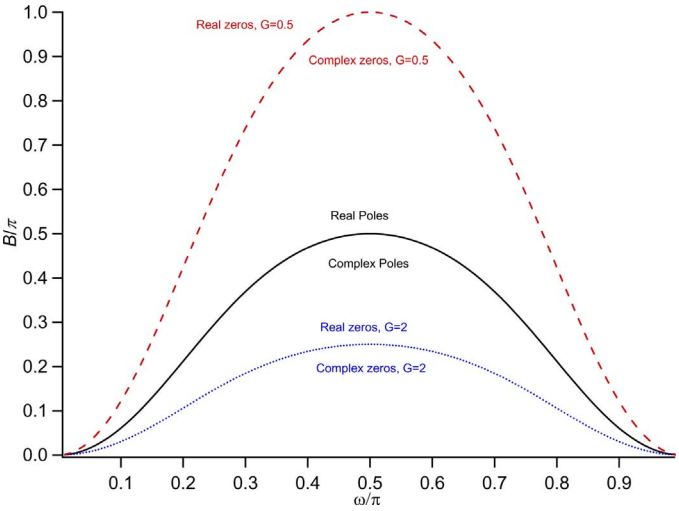

Fig. 4. Boundaries between regions where the preferred solution has real or complex zeros for $G = 0.5$ and $G = 2$. The boundaries between regions where poles are real or complex is also shown, and is independent of G.

If we assume the poles or zeros are complex conjugate pairs, then the conditions for stability and minimum phase behavior may be found from the pole and zero radii:

$$\begin{aligned} 0 < r_z^2 < 1 &\rightarrow -\alpha < \beta G < 0 \\ 0 < r_p^2 < 1 &\rightarrow 0 < \pm_c \beta < \alpha. \end{aligned} \tag{26}$$

Since the gain is positive, β must be negative. So the negative sign is used in $\beta = \pm\tan(B/2)$, and the negative sign is used in $\pm_c$.

Without loss of generality, assume that bandwidth has been defined using the arithmetic mean ($\alpha = 1$). The regions with complex or real valued poles and zeros are depicted in Fig. 4 for $G = 0.5$ and $G = 2$. It can be seen that real valued poles or zeros only exist for large values of bandwidth as compared to the center frequency. This is an unusual situation, since the notch and peaking filters are generally cascaded such that each filter acts on a relatively narrow range of frequencies.

Our preferred solution for the parametric equalizer gives poles and zeros as

$$r_z e^{\pm j\omega_z} = \frac{\cos\omega_c}{1+G\tan\left(\frac{B}{2}\right)} \pm j\frac{\sqrt{\sin^2\omega_c - G^2\tan^2\left(\frac{B}{2}\right)}}{1+G\tan\left(\frac{B}{2}\right)}$$
$$r_p e^{\pm j\omega_p} = \frac{\cos\omega_c}{1+\tan\left(\frac{B}{2}\right)} \pm j\frac{\sqrt{\sin^2\omega_c - \tan^2\left(\frac{B}{2}\right)}}{1+\tan\left(\frac{B}{2}\right)}. \quad (27)$$

We define an angle θ_p such that

$$\cos\theta_p = -\frac{\sin^2\omega_c + \tan\left(\frac{B}{2}\right)}{\left[1+\tan\left(\frac{B}{2}\right)\right]\sin\omega_c},$$
$$\sin\theta_p = \frac{\cos\omega_c\sqrt{\sin^2\omega_c - \tan^2\left(\frac{B}{2}\right)}}{\left[1+\tan\left(\frac{B}{2}\right)\right]\sin\omega_c}. \quad (28)$$

This is valid since $\cos^2\theta_p + \sin^2\theta_p = 1$, and the square root term in (28) is real for complex poles. Similarly, we define

$$\cos\theta_z = -\frac{\sin^2\omega_c + G\tan\left(\frac{B}{2}\right)}{\sin\omega_c\left[1+G\tan\left(\frac{B}{2}\right)\right]},$$
$$\sin\theta_z = \frac{\cos\omega_c\sqrt{\sin^2\omega_c - G^2\tan^2\left(\frac{B}{2}\right)}}{\sin\omega_c\left[1+G\tan\left(\frac{B}{2}\right)\right]}. \quad (29)$$

Then, it can be easily shown that

$$r_p e^{\pm j\omega_p} = \sec\omega_c + \tan\omega_c e^{\pm j\theta_p}$$
$$r_z e^{\pm j\omega_z} = \sec\omega_c + \tan\omega_c e^{\pm j\theta_z}. \quad (30)$$

Thus, all solutions with constant frequency lie on the circle defined by the center $\sec(\omega_c)$ and radius $\tan(\omega_c)$. The position of the poles is independent of the gain, and the position of the zeros is on the same circle, but with displacement from the poles dependent on the gain.

Now note that the pole radius and zero radius may be given as follows:

$$r_p = \sqrt{\frac{1-\tan\left(\frac{B}{2}\right)}{1+\tan\left(\frac{B}{2}\right)}}, r_z = \sqrt{\frac{1-G\tan\left(\frac{B}{2}\right)}{1+G\tan\left(\frac{B}{2}\right)}}. \quad (31)$$

That is, all poles lie on the curve with center at zero, and radius given only as a function of bandwidth. The zeros lie on different curves, given by both the gain and the bandwidth. We have thus defined curves of constant frequency for poles and zeros, curves of constant bandwidth for poles, and curves of constant gain and bandwidth for zeros. These curves are depicted in Fig. 5, for both bandwidth and center frequency ranging from 0.05π to 0.45π in units of 0.05π. One can see the relationship between varying the parametric equalizer parameters and movement of the poles and zeros on the complex plane.

V. Conclusion

In this paper, we presented an exact derivation of the parametric equalizer without resorting to an analog prototype or any approximations. We showed that there are actually 32 possible solutions to the parametric equalizer design constraints as usually stated. There are two reasons for this. The first is that the bandwidth is usually given only in terms of the distance between upper and lower cutoff frequencies, but does not specify where they are placed. The second reason is that the constraints allow for unstable or nonminimum phase solutions. Only one solution consistently yields stable, mimimum phase behavior with the upper and lower cutoff frequencies positioned around the center frequency. The resultant pole zero placements were examined, including the conditions for poles or zeros existing in complex conjugate pairs, and the effect of moving poles or zeros in the complex plane.

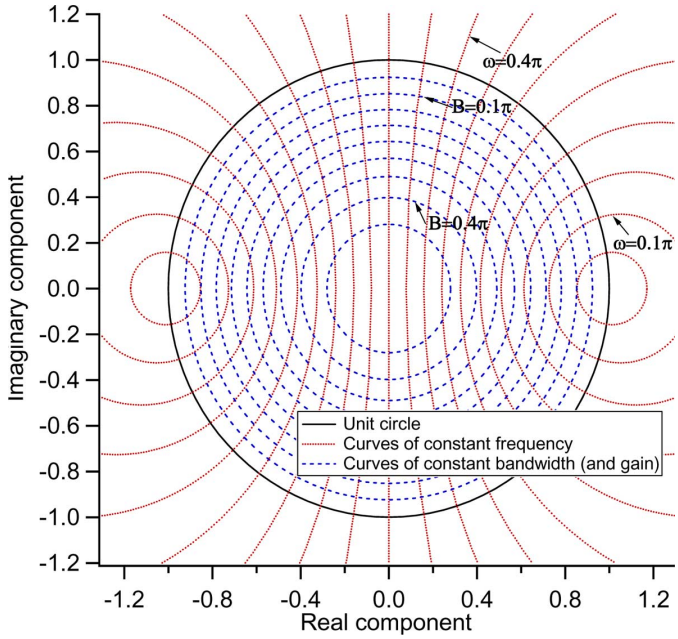

Fig. 5. Curves of constant frequency and curves of constant bandwidth and gain depicted on the complex plane. The dotted curves represent the locations of zeros and poles while holding frequency constant and varying gain or bandwidth. The dashed curves represent the locations of poles while holding frequency constant and varying gain or bandwidth. The locations of zeros for fixed frequency and fixed gain are on the same dashed curves, but have a modified radius if gain is varied.

The approach given here used trigonometric relationships to determine filter parameters directly from the conditions which specify the filter design. Although the analysis was fairly detailed, if one only wishes to derive the ideal solution, then the complexity of this technique is fairly small. Case 1.2 and Case 2 of Section II may be ignored, as well as all the alternative solutions for β and the different choices for the $\pm$ signs. Thus, this derivation may be considered as simple as those based on transformation of analog prototypes, if not simpler. It offers the advantage of being able to work only in the z domain, as opposed to both the z domain and the Laplace domain. Nor does it require one to transform an allpass filter, as suggested in [3], [14], [16], or involve any of the approximations previously described. Furthermore, although the technique began with the filter described in pole zero form without the assumption of complex conjugate poles or zeros, the same approach could have been applied to derive the coefficients of the direct form or the radii and angles of complex conjugate pole zero pairs.

A similar approach could be taken to design other second-order digital filters often given as parametric structures, such as low-pass, high-pass, band-pass, and shelving filters. Fully digital IIR filter design techniques may also lead to new digital filters which need not be directly related to existing analog prototypes. This is the author's direction of future research in this area.

Acknowledgment

The author would like to thank P. Eastty, U. Zolzer, and R. Bristow-Johnson for their insightful comments during the preparation of this manuscript.

References

[1] L. R. Rabiner and B. Gold, *Theory and Application of Digital Signal Processing*. Englewood Cliffs, NJ: Prentice-Hall, 1975.
[2] R. A. Losada and V. Pellisier, "Designing IIR filters with a given 3-dB point," *IEEE Signal Process. Mag.*, vol. 22, no. 4, pp. 95–98, Jul. 2005.
[3] U. Zolzer, *Digital Audio Signal Processing*, 2nd ed. New York: Wiley, 2008.

[4] S. J. Orfanidis, "High-order digital parametric equalizer design," *J. Audio Eng. Soc.*, vol. 53, pp. 1026–1046, Nov. 2005.
[5] J. A. Moorer, "The manifold joys of conformal mapping: Applications to digital filtering in the studio," *J. Audio Eng. Soc.*, vol. 31, pp. 826–841, Nov. 1983.
[6] S. A. White, "Design of a digital biquadratic peaking or notch filter for digital audio equalization," *J. Audio Eng. Soc.*, vol. 34, pp. 479–483, Jun. 1986.
[7] P. A. Regalia and S. K. Mitra, "Tunable digital frequency response equalization filters," *IEEE Trans. Acoust., Speech, Signal Process.*, vol. ASSP-35, no. 1, pp. 118–120, Jan. 1987.
[8] D. C. Massie, "An engineering study of the four-multiply normalized ladder filter," *J. Audio Eng. Soc.*, vol. 41, pp. 564–582, Jul./Aug. 1986.
[9] R. Bristow-Johnson, "The equivalence of various methods of computing biquad coefficients for audio parametric equalizers," in *Proc. 97th Audio Eng. Soc. Conv.*, San Francisco, CA, 1994.
[10] K. B. Christensen, "A generalization of the biquadratic parametric equalizer," in *Proc. 115th Audio Eng. Soc. Conv.*, New York, 2003.
[11] S. J. Orfanidis, "Digital parametric equalizer design with prescribed Nyquist frequency gain," *J. Audio Eng. Soc.*, vol. 45, pp. 444–455, 1997.
[12] A. Fernandez-Vazquez and G. Jovanovic-Dolecek, "A new method for the design of IIR filters with flat magnitude response," *IEEE Trans. Circuits Syst. I: Regular Papers*, vol. 53, no. 8, pp. 1761–1771, Aug. 2006.
[13] C.-C. Tseng and S.-C. Pei, "Stable IIR notch filter design with optimal pole placement," *IEEE Trans. Signal Process.*, vol. 49, no. 11, pp. 2673–2681, Nov. 2001.
[14] A. Fernandez-Vazquez *et al.*, "A new method for designing flat shelving and peaking filters based on allpass filters," in *Proc. 17th Int. Conf. Electron., Commun. Comp. (CONIELECOMP'07)*, Cholula, Mexico, 2007.
[15] S. Yimman *et al.*, "IIR multiple notch filters design with optimum pole position," in *Proc. IEEE Int. Conf. Commun. Inf. Technol. (ISCIT-06)*, Bangkok, Thailand, 2006, pp. 281–286.
[16] S.-C. Pei and C.-C. Tseng, "IIR multiple notch filter design based on allpass filter," *IEEE Trans. Circuits Syst. II: Analog Digital Signal Process.*, vol. 44, no. 2, pp. 133–136, Feb. .
[17] T. v. Waterschoot and M. Moonen, "A pole-zero placement technique for designing second-order IIR parametric equalizer filters," *IEEE Trans. Audio, Speech Lang. Process.*, vol. 15, no. 8, pp. 2561–2565, Nov. 2007.